


Astrocyte Glutamate Uptake and Water Homeostasis Are Dysregulated in the Hippocampus of Multiple Sclerosis Patients With Seizures

Andrew S. Lapato^{1,2}, Sarah M. Thompson¹, Karen Parra¹ and Seema K. Tiwari-Woodruff^{1,2,3} 

ASN Neuro
Volume 12: 1–15
© The Author(s) 2020
Article reuse guidelines:
sagepub.com/journals-permissions
DOI: 10.1177/1759091420979604
journals.sagepub.com/home/asn


Abstract

While seizure disorders are more prevalent among multiple sclerosis (MS) patients than the population overall and prognosticate earlier death & disability, their etiology remains unclear. Translational data indicate perturbed expression of astrocytic molecules contributing to homeostatic neuronal excitability, including water channels (AQP4) and synaptic glutamate transporters (EAAT2), in a mouse model of MS with seizures (MS+S). However, astrocytes in MS+S have not been examined. To assess the translational relevance of astrocyte dysfunction observed in a mouse model of MS+S, demyelinated lesion burden, astrogliosis, and astrocytic biomarkers (AQP4/EAAT2/ connexin-CX43) were evaluated by immunohistochemistry in postmortem hippocampi from MS & MS+S donors. Lesion burden was comparable in MS & MS+S cohorts, but astrogliosis was elevated in MS+S CA1 with a concomitant decrease in EAAT2 signal intensity. AQP4 signal declined in MS+S CA1 & CA3 with a loss of perivascular AQP4 in CA1. CX43 expression was increased in CA3. Together, these data suggest that hippocampal astrocytes from MS+S patients display regional differences in expression of molecules associated with glutamate buffering and water homeostasis that could exacerbate neuronal hyperexcitability. Importantly, mislocalization of CA1 perivascular AQP4 seen in MS+S is analogous to epileptic hippocampi without a history of MS, suggesting convergent pathophysiology. Furthermore, as neuropathology was concentrated in MS+S CA1, future study is warranted to determine the pathophysiology driving regional differences in glial function in the context of seizures during demyelinating disease.

Keywords

demyelination, epilepsy, neuropathology

Received July 20, 2020; Revised October 6, 2020; Accepted for publication October 26, 2020

Multiple sclerosis (MS) is an autoimmune demyelinating disease of the central nervous system (CNS) that affects roughly 913,925 in the United States (Wallin et al., 2019). Neurological symptomatology in MS is multifarious, owing to the largely non-stereotyped distribution of leukocytic lesions throughout the brain and spinal cord of MS patients. In addition to the loss of myelin at the site of autoimmune attack, denuded axons within the lesion undergo various deleterious changes (Trapp et al., 1998; Nave & Trapp, 2008), producing deficits in autonomic, cognitive, motor, sensory, and visual function (Rosenthal et al., 2020). While these outcomes are well-characterized, epileptic seizures are observed at a rate three times higher in MS patients than the population

overall for reasons that are incompletely understood (Poser & Brinar, 2003; Catenoix et al., 2011).

¹Division of Biomedical Sciences, UCR School of Medicine, Riverside, California, United States

²Center for Glial-Neuronal Interaction, UCR School of Medicine, Riverside, California, United States

³Department of Neuroscience, UCR School of Medicine, Riverside, California, United States

Corresponding Author:

Seema K. Tiwari-Woodruff, Division of Biomedical Sciences, School of Medicine, University of California Riverside, Rm 3140, Multidisciplinary Research Building, 900 University Ave, Riverside, CA 92521, United States. Email: seema.tiwari-woodruff@medsch.ucr.edu



Both partial and generalized seizures are commonly identified in MS patients with seizure disorders (MS+S), although primary and secondary generalized subtypes account for approximately 67% of cases (Moreau et al., 1998; Nyquist et al., 2001; Spatt et al., 2001; Koch et al., 2008; Shaygannejad et al., 2013). Unusual seizure manifestations are also reported by these patients, including dysphasic/aphasic status epilepticus and musicogenic seizures (Newman & Saunders, 1980; Spatt et al., 1994; Primavera et al., 1996). Seizures may herald or occur contemporaneous to relapse in a subset of MS+S patients (Kelley & Rodriguez, 2009; Catenox et al., 2011; Shaygannejad et al., 2013; Lund et al., 2014; Uribe-San-Martin et al., 2014) and rise in incidence with disease duration (Striano et al., 2003; Martínez-Juárez et al., 2009; Lund et al., 2014; Colasanti et al., 2016). Although their etiology remains unclear, seizures in MS are associated with poor response to traditional anti-epileptic drugs (AEDs), which may precipitate relapse-like symptoms, worsen neurological dysfunction, or engender seizures (Moreau et al., 1998; Solaro et al., 2005; Catenox et al., 2011; Colasanti et al., 2016; Burman & Zelano, 2017). While seizures in MS produce significantly worse health outcomes and are poorly controlled by AEDs, their pathophysiology and risk factors are poorly understood.

Though limited in number, paraclinical studies examining MS+S have yielded some insight into distinguishing features of seizures arising during MS. MS patients with seizures exhibit a variety of electroencephalographic (EEG) abnormalities that localize to structures associated with seizure in temporal lobe epilepsy, suggesting commonality between the two disorders. In addition to a varying degree of diffuse slowing across monitored sites, EEG recordings from MS+S patients display sharp- and slow-wave complexes, high amplitude delta waves, and rhythmic interictal discharges in frontotemporal areas (Ghezzi et al., 1990; Moreau et al., 1998; Striano et al., 2003; Martínez-Lapiscina et al., 2013). In addition to possessing possible diagnostic value, these studies confirm that seizures in MS patients are electrographically identifiable and may follow a similar course of disease.

Magnetic resonance imaging (MRI) studies examining cortical structures showing EEG irregularities in MS+S patients have identified differences in lesion phenotype and distribution relative to MS patients without seizures. Along with abundant grey matter lesions (GMLs), large cortical lesions that extend across adjacent gyri are observed in MS+S more frequently than other MS patients (Calabrese et al., 2008, 2012). Subcortical areas are similarly affected in MS+S: limbic structures implicated as seizure foci in patients with temporal lobe epilepsy display significant damage, including accumulation

of enhancing lesions in the hippocampal formation, cingulate cortex, and insula (Calabrese et al., 2017). In addition to showing temporal lobe atrophy that outpaces other cortical areas, MS+S hippocampi harbor nearly four times as many GMLs than MS only, with similarly high ratios observed in abutting structures (Calabrese et al., 2017). While these studies support a role for enhanced inflammatory lesion burden in MS patients with seizures, their ability to clarify the cellular mechanism driving seizures in MS is limited. Thus, direct observation of possible cellular and molecular players in the etiology of MS+S is warranted.

Immunohistochemical examination of postmortem MS+S brain tissue supports may provide some insight into the mechanism driving seizures in MS. In a cohort of postmortem specimens from the United Kingdom MS Tissue Bank, Nicholas et al. observed that the number of GABAergic neurons, identified by immunoreactivity for the GABA synthetic enzyme glutamate decarboxylase (GAD)67, was reduced in layers IV & VI of the middle temporal gyrus of MS+S donors relative to MS only donors (Nicholas et al., 2016). Interestingly, this study also showed that loss of GABAergic populations is independent of local leukocytic infiltration or compromised cellular respiration, leaving the etiology of GABAergic cell loss in MS+S uncertain (Nicholas et al., 2016). These findings are analogous to temporal lobe epilepsy (TLE) and are thought to facilitate the initiation and spread of seizures (de Lanerolle et al., 2012; Huusko et al., 2015), suggesting that MS+S involves similar disinhibition of neocortical circuits.

Translational studies point to a second possible avenue by which neuronal excitability may be dysregulated in MS+S. Concomitant to loss of GABAergic neurons, mice with demyelination-induced seizures display marked hippocampal astrogliosis with perturbed expression of the astrocyte water channel aquaporin (AQP)4 (Lapato et al., 2017). Although the specific contribution of AQP4 to seizures is complex and not fully delineated, these observations mirror a growing body of literature implicating astrocytes in the pathophysiology of epilepsy. Astrocyte processes critical to the maintenance of normal neuronal excitation are disordered in epilepsy, including impaired regulation of synaptic glutamate, disruption of water homeostasis, and delayed clearance of extracellular K^+ (Bergles & Jahr, 1998; Eid et al., 2005; Takahashi et al., 2010; Lee et al., 2012a; Alvestad et al., 2013; Coulter & Steinhauser, 2015). Several of these are critically mediated by gap junction coupling among astrocytes linked into a glial syncytium, leading at least one group to indict astrocyte uncoupling in the etiology of epileptic seizures (Tress et al., 2012; Bedner & Steinhauser, 2013; Chever et al., 2014b; Bedner et al., 2015; Lapato & Tiwari-Woodruff, 2018). Yet as TLE pathophysiology involves myriad cellular and molecular

actors, the degree to which TLE & MS+S neuropathology converges has not been established.

Here, we examine astrocyte dysfunction in a cohort of postmortem hippocampal tissue from MS patients with and without seizures obtained from the NIH NeuroBioBank/Human Brain & Spinal Fluid Resource Center (HBSFRC) brain bank at the University of California Los Angeles (UCLA). Specifically, we examined expression of astrocyte-derived molecules involved in homeostatic neuronal excitability that are impacted in epilepsy as well as demyelination extent. These targets include the water channel AQP4, the relevance of which is noted above, the primary synaptic glutamate transporter in the adult mammalian CNS, excitatory amino acid transporter (EAAT)2 (Holmseth et al., 2009; Rimmelé & Rosenberg, 2016), and the primary astrocyte-expressed gap junction component protein, connexin (CX)43.

Our data suggest that, while demyelination was comparable in the HBSFRC cohort, astrocytes displayed marked changes in the MS+S group, including reduced clearance of synaptic glutamate, impaired water & potassium (K^+) buffering, and altered gap junction coupling between astrocytes. As new, more efficacious interventions are necessary for the management of MS+S, this study lays the groundwork for further translational study probing the contribution of astrocytes to demyelination-induced seizures.

Materials and Methods

Human Postmortem Hippocampal Specimens

Human tissue was acquired from the NIH NeuroBioBank/HBSFRC at UCLA with a history of MS and MS preceding seizure disorder diagnosis. Tissues arrived with limited cause of death and neuropathology reports with all identifying patient data removed. EDSS scores or frequency of seizures was not disclosed in specimen information provided. Donor age at death, autolysis time, and cohort gender composition and more detailed information is presented in Table 1 and Supplemental Table. Due to anatomical variability in HBSFRC samples, not all sections contained all hippocampal subregions analyzed, leading to *n* values below cohort totals.

Immunohistochemistry

Tissues were received from HBSFRC frozen, whereupon they were gradually thawed at 4°C followed by two hours fixation in 10% neutral buffered formalin (Fisher Scientific, Hampton, NH) at the same temperature. Following incubation, specimens were cryoprotected in 30% w/v sucrose in phosphate buffered saline (PBS)

with 0.2% w/v NaN_3 (both Millipore Sigma, St. Louis, MO) and incubated at 4°C until tissue density exceeded that of the sucrose solution. Once cryoprotection was complete, specimens were embedded in Tissue-Tek Cryo-OCT compound (Andwin Scientific, Los Angeles, CA) and 40 μ m sections were cut using an HM525 cryostat (Thermo Fisher Scientific, Waltham, MA) and stored in PBS with 0.1% w/v NaN_3 4°C until use.

40 μ m free floating postmortem hippocampal specimens were immunostained following a previously described procedure (Hasselmann et al., 2017; Mangiardi et al., 2011). All antibodies & dilutions used in the present study are denoted in Table 2 (obtained from Millipore Sigma & Invitrogen, Carlsbad, CA). Primary antibodies were diluted in PBS and detection antibodies were diluted in tris-buffered saline (TBS). For chromogen myelin labeling, after incubation with horseradish peroxidase (HRP)-conjugated detection antibody, MOG immunoreactivity was visualized using the 3,3'-diaminobenzidine (DAB) Peroxidase (HRP) Substrate Kit (Vector Laboratories, Burlingame, CA), mounted to slides, counterstained with Hematoxylin QS (Vector Laboratories), then cover-slipped using Permount non-aqueous medium (Fisher Scientific). For fluorescent microscopy, after incubation with fluorophore-conjugated antibodies, sections were counterstained in TBS containing 4',6-diamidino-2-phenylindole (DAPI, 2 ng/ml; Molecular Probes), mounted on glass slides, and cover-slipped in Fluoromount G aqueous medium (Thermo Fisher Scientific).

Imaging and Quantification

Chromogen-stained hippocampi were imaged using a Leica DM5500 B upright transmitted light microscope (Leica Microsystems Inc., Buffalo Grove, IL) at 5X magnification, then stitched into segments using a pairwise-stitching algorithm (Preibisch et al., 2009) included with the Fiji ImageJ package (Schindelin et al., 2012), and segments were assembled in Adobe Illustrator (Adobe Inc., San Jose, CA). Fluorescence micrographs were acquired on an Olympus BX61 confocal microscope (Olympus America Inc., Center Valley, PA) at 20X magnification. $\leq 20 \mu$ m thick z-stack projections were compiled using SlideBook 6 software (Intelligent Imaging Innovations, Inc., Denver, CO) or Olympus cellSens software (Olympus America Inc.).

Image analysis was carried out in Fiji software. Data points represent average values for two fields of view per area per donor sample. Fields were selected away from active lesions and large white matter tracts to assess normal appearing gray matter, equating to stratum radiatum in CA1 & CA3 and hilus in DG. Lesion density was calculated by delineating rough lesion borders in stitched images then normalizing lesion counts to total area

Table 1. Summary of Patient Demographics of Specimens Acquired From HBSFRC.

| Disease | n | MS phenotype | Age at death (yrs±SD) | Autolysis time (hrs±SD) |
|---------|----------------|----------------|-----------------------|-------------------------|
| MS only | 21 (12 ♀, 9 ♂) | MS, RRMS, SPMS | 65.6 ± 9.3 | 16.4 ± 7.5 |
| MS+S | 7 (4 ♀, 3 ♂) | MS, SPMS | 61.9 ± 13.3 | 20.3 ± 10.1 |

SD = standard deviation, MS = multiple sclerosis, RRMS = relapsing-remitting MS, SPMS = secondary progressive MS.

Table 2. Primary and Detection Antibodies Utilized With Manufacturer Information and Concentration Used.

| Antibody | Manufacturer | Catalogue # | RRID | Dilution |
|--|-----------------|-------------|-------------|----------|
| mouse anti-myelin oligodendrocyte glycoprotein (MOG) | Millipore Sigma | MAB5680 | AB_1587278 | 1:500 |
| chicken anti-glial fibrillary acidic protein (GFAP) | Millipore Sigma | AB5541 | AB_177521 | 1:1000 |
| rabbit anti-aquaporin-4 (AQP4) | Millipore Sigma | AB2218 | AB_1163383 | 1:500 |
| guinea pig anti-glutamate transporter, glial (EAAT2) | Millipore Sigma | AB1783 | AB_90949 | 1:1000 |
| rabbit anti-connexin 43 (CX43) | Millipore Sigma | C6219 | AB_476857 | 1:500 |
| goat anti-mouse IgG (H + L), horseradish peroxidase | Millipore Sigma | AP308P | AB_11215796 | 1:500 |
| goat anti-chicken Ig (H + L), DyLight 650 | Invitrogen | SA5-10073 | AB_2556653 | 10 µg/mL |
| goat anti-rabbit IgG (H + L), Alexa Fluor +555 | Invitrogen | A32732 | AB_2633281 | 1:500 |
| goat anti-rabbit IgG (H + L), Alexa Fluor +488 | Invitrogen | A32731 | AB_2633280 | 1:500 |
| goat anti-rabbit IgG (H + L), Cy3 | Millipore Sigma | API08C | AB_92422 | 1:500 |

within each of the 3 subregions analyzed. Signal intensity (mean gray value) was measured in regions of interest containing CA1/CA3 stratum radiatum and pyramidal cell layer or hilus/CA4 for DG and normalized to minimum/maximum values for the entire HBSFRC cohort.

Statistical Analysis

Statistical analysis was carried out per previously published work (Tiwari-Woodruff et al., 2007; Crawford et al., 2010). All statistics were performed using Prism 8 software (GraphPad Software, La Jolla, CA). Differences were considered significant at $p \leq 0.05$ and denoted by the addition of an asterisk (*) above the statistically different data sets. All statistical tests used to determine significance are noted in corresponding figure legends. *N* values included in each analysis are represented as individual points in scatter plots shown. Anatomical variation within HBSFRC tissues circumscribed the number of specimens available for DG analysis, leading to reduced data points within those plots.

Results

Donor Demographic Data and Characteristics of Specimens Obtained from the HBSFRC

Hippocampi from 21 MS and 7 MS+S donors were obtained from the HBSFRC (Table 1). The MS only

cohort was 57.1% female and 42.9% male and was composed of donors with relapsing-remitting MS (RRMS; 23.8%), secondary progressive (SPMS; 33.3%), and non-specified MS (42.9%) disease phenotypes. Average age at death for this group was 64.6 ± 10.5 & 66.9 ± 7.9 years for female and male donors, respectively, and a cohort average of 65.6 ± 9.3 . Autolysis time was comparable between male (14.7 ± 8.9 hours) and female (27.6 ± 6.3 hours) specimens, with an aggregate average of 16.4 ± 7.5 hours. Neither age at death ($p = 0.5871$) or autolysis time ($p = 0.3807$) were statistically different between male and female donors within the MS only group.

The MS+S cohort was divided equally between female and male donors, with 42.9% of donors diagnosed with SPMS and 57.1% having an unspecified MS phenotype. Female donors were aged 59.8 ± 15.9 years at time of death and male donors 64.8 ± 11.6 , for a cohort average of 61.9 ± 13.4 years. On average, female specimens waited 14.6 ± 3.6 hours and male specimens 27.9 ± 11.6 hours until cryopreservation (cohort average = 20.3 ± 10.1 hours). No differences were identified in age at death ($p = 0.6722$) or autolysis time ($p = 0.0763$) between male and female specimens in the MS+S cohort.

No differences were observed in age at death ($p = 0.4195$) or autolysis time ($p = 0.2829$) when comparing MS and MS+S groups overall or when divided by sex (male: age at death $p = 0.7112$, autolysis time $p = 0.0636$; female: age at death $p = 0.4912$, autolysis time $p = 0.3727$).

Brain Slice Integrity and Identifications of Structures to Compare

Initially, slices from all postmortem specimens were Nissl stained to assess tissue integrity and delineate anatomical boundaries of subregions. Most, but not all, slices displayed coronally sectioned hippocampal formation with some abutting structures as depicted in Figure 1 schematic drawing. Cornu Ammonis (CA)1, CA3 and dentate gyrus (DG) were identified based on cytoarchitecture (Figure 1A to C) and mapped for subsequent analysis and comparison. These subregions were chosen as they represent most major functionally distinct gray matter structures participating in the hippocampal trisynaptic circuit (Wojtowicz, 2012) and frequently display pathological changes in epilepsy (de Lanerolle et al., 2012). DG was either only partially represented or absent in approximately 1/3rd of samples. CA1 & CA3 were analyzed in these specimens but no data was acquired for DG comparisons.

MS and MS+S Hippocampi Obtained from the HBSFRC Display Similar Demyelinated Lesion Burden

Imaging studies report greater numbers of demyelinating lesions in the hippocampi of MS+S patients relative to MS patients without seizures (Calabrese et al., 2017). To establish whether the HBSFRC cohort displays similar differences in myelination, immunolabeling for myelin oligodendrocyte glycoprotein (MOG) was performed and the density of lesions in CA1, CA3, and DG were measured (Figure 2).

Demyelinated lesions were observed in both MS & MS+S groups that varied in their size and involvement of adjacent structures (Figure 2A). Quantification of lesion density in hippocampal subregions revealed no difference in lesion burden in CA1, CA3, or DG between MS & MS+S specimens in the HBSFRC cohort (Figure 2B to D).

GFAP⁺ Astrogliosis is More Pronounced in the CA1 Subfield of MS Patients with Seizures

Astroglia, identified by proliferation of astrocytes and upregulation of the intermediate filament GFAP, is a commonly observed feature of various neurological diseases, including MS and epilepsy (de Lanerolle et al., 2012; Brosnan & Raine, 2013). Reactive astrocytes undergo changes to their metabolism and physiology that exacerbate disease severity and could facilitate seizures, including attenuation of glutamate transporter activity (Vercellino et al., 2007; Azevedo et al., 2014), release of reactive O₂/N₂ species (Gavillet et al., 2008), and loss of gap junction coupling-mediated K⁺ homeostasis (Bedner et al., 2015; Karim et al., 2018). Thus, to

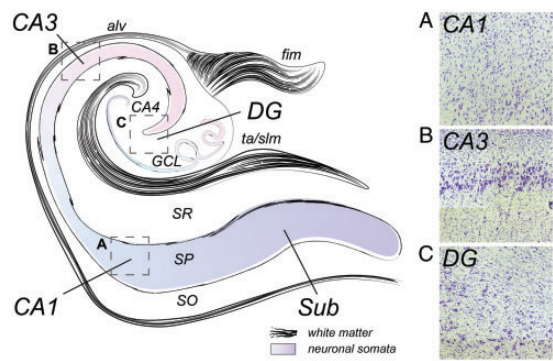


Figure 1. Illustrated human hippocampal anatomy and cytoarchitecture characteristic of CA1, CA3, & DG images used for analysis. Diagram shows human hippocampus with subiculum (Sub), CA1, CA3, CA4, and dentate gyrus (DG) with strata oriens (SO), pyramidal (SP), radiatum (SR), and lacunosum-moleculare, as well as granule cell layer (GCL), noted. Dashed boxes correspond to representative 5X Nissl stained cytoarchitecture (shown in insets A–C) used to identify regions for DG confocal imaging.

identify differences in the extent of astroglia between MS & MS+S specimens, GFAP⁺ immunoreactivity was assessed in CA1, CA3, and DG subfields.

GFAP⁺ signal intensity was elevated in MS+S CA1 relative to MS only (Figure 3A and B). No difference in GFAP⁺ signal intensity was observed in CA3 or DG subfields (Figure 3C to F). No difference was observed in the total GFAP⁺ immunoreactive area fraction between MS & MS+S in any region (not shown), suggesting increased signal intensity was not due to differences in number of GFAP⁺ cells or coverage of GFAP⁺ processes.

Reduced AQP4 Expression in MS+S CA1 and CA3 Subregions with Loss of Vascular Localization

The glial water channel AQP4 is thought to play a role in maintenance of extracellular space volume and facilitation of ion movement throughout cytoplasmically linked glial networks (Binder et al., 2006; Strohschein et al., 2011). Perturbation of AQP4 expression and localization away from its normal perivascular distribution is commonly observed in hippocampi of epileptic patients (Lee et al., 2004; Eid et al., 2005) as well as in experimental models (Lee et al., 2012b; Alvestad et al., 2013; Hubbard et al., 2016). To assess whether MS+S involves similar changes to AQP4, its expression was evaluated in MS & MS+S hippocampi.

Relative to MS only, MS+S CA1 and CA3 exhibited reduced AQP4 staining intensity (Figure 4A and B, D and E). No statistically significant difference was observed in MS+S DG (Figure 4C and F), although AQP4 immunoreactive area fraction trended toward increase in MS+S DG (not shown, $p=0.0605$). Of

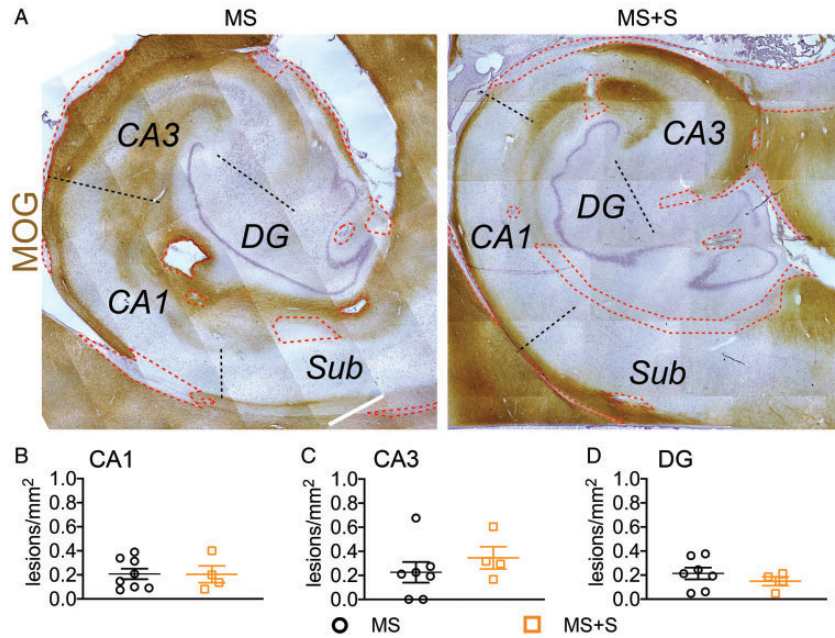


Figure 2. Demyelinated lesion burden is similar in the HBSFRC cohort. A: Representative 5X stitched micrographs showing MOG immunoreactivity in MS & MS+S hippocampus visualized by HRP-DAB chromogen immunohistochemistry with hematoxylin counterstain. CA1, CA3, DG, & Sub are indicated. Demyelinated lesions are traced by red dashed line. Black dashed lines represent divisions between subregions. B–D: Quantification of lesion distribution in MS & MS+S tissues. Comparison of demyelinated lesion density in CA1 (B), CA3 (C), and DG (D) revealed no significant difference in lesion burden between MS & MS+S specimens. Unpaired t-test.

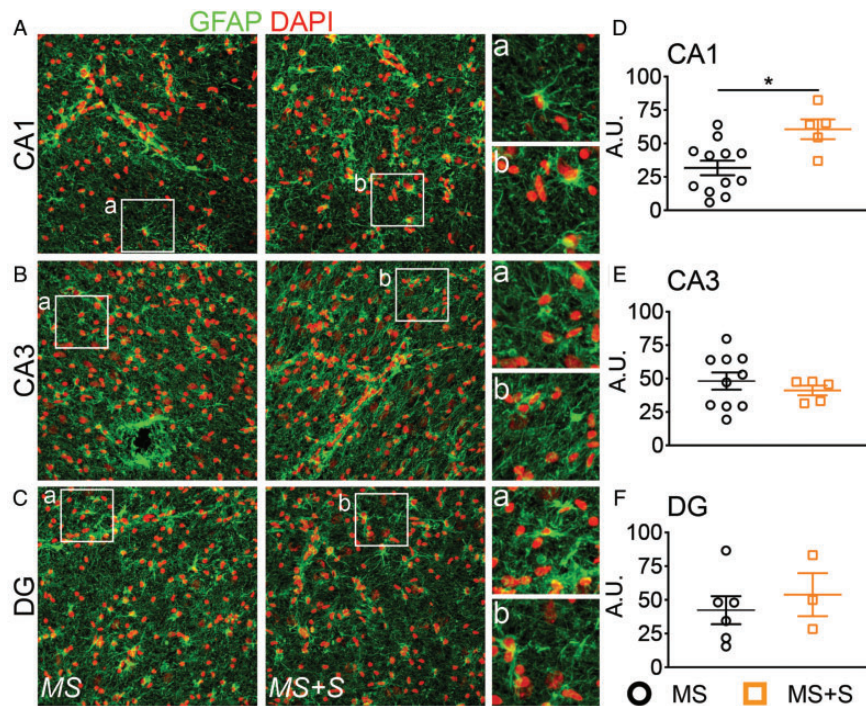


Figure 3. GFAP⁺ astroglial signal intensity is more pronounced in the CA1 subfield of MS patients with seizures. A–C: Representative 20X micrographs showing astrocytes (GFAP; green) with nuclear counterstain (DAPI; red) in CA1, CA3, & DG of MS & MS+S hippocampi. Insets a and b show digitally magnified area within dashed boxes for detail. D–F) Normalized GFAP immunoreactive signal intensity in MS & MS+S CA1 (D), CA3 (E), and DG (F) is shown in arbitrary units (A.U.). Relative to MS, GFAP⁺ signal intensity was greater in CA1 of MS+S specimens. No difference was observed in CA3 or DG. Unpaired t test.

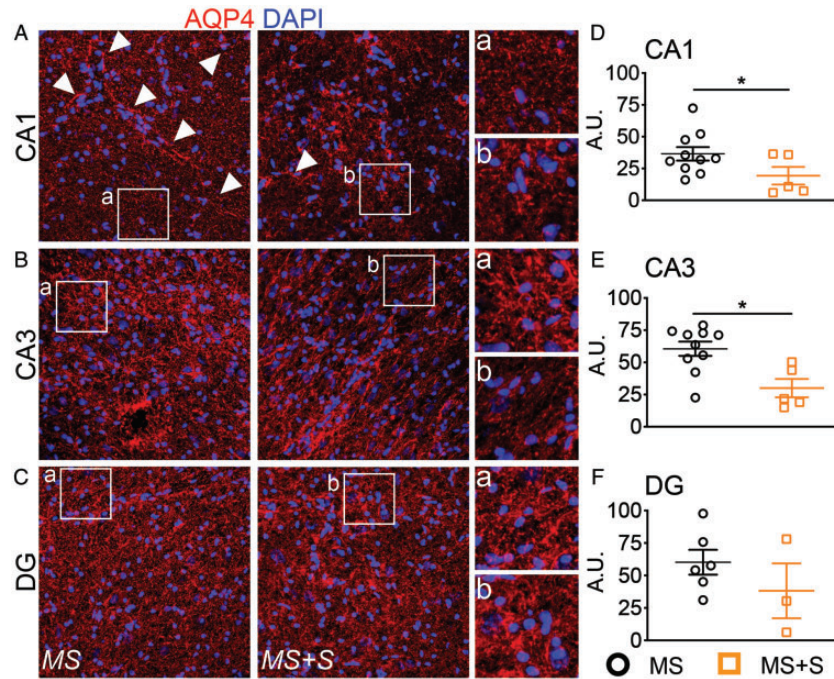


Figure 4. AQP4 expression is decreased in MS+S CA1 & CA3 subregions with loss of perivascular localization in the HBSFRC cohort. A–C: Representative 20X micrographs showing AQP4 (red) with nuclear counterstain (DAPI; blue) in CA1, CA3, & DG of MS & MS+S hippocampi. Insets a and b show digitally magnified area within dashed boxes for detail. Note reduced perivascular AQP4 localization in MS+S CA1 (arrowheads). D–F: Normalized GFAP immunoreactive signal intensity in MS & MS+S CA1 (D), CA3 (E), and DG in shown in arbitrary units (A.U.). Relative to MS, AQP4 expression was reduced in MS+S CA1 & CA3. No difference was observed in DG. Unpaired t test.

interest, while AQP4 signal was enriched proximal to putative blood vessels in MS CA1, perivascular AQP4 staining was infrequent in MS+S CA1 (Figure 4A, arrowheads). No differences were noted in perivascular AQP4 in CA3 and DG.

Synaptic Glutamate Clearance Is Likely Impaired in the CA1 of MS+S Specimens Obtained From HBSFRC

The glial glutamate/aspartate transporter EAAT2 is the most widely distributed glutamate transporter in the adult mammalian brain (Lehre & Danbolt, 1998). As regional loss of glutamate transporters and accumulation of extracellular glutamate is observed in both MS and temporal lobe epilepsy (Mathern et al., 1999; Werner et al., 2001; Proper et al., 2002; Vercellino et al., 2007; Azevedo et al., 2014), differences in EAAT2 immunostaining were assessed in MS & MS+S hippocampi.

EAAT2 staining intensity was diminished in MS+S CA1 relative to MS only (Figure 5A and D). In contrast, no statistically significant difference was observed in EAAT2 signal strength in CA3 (Figure 5B and E) or DG (Figure 5C and F). However, while EAAT2 immunoreactive area fraction was not statistically different in CA1 or CA3 subregions, EAAT2⁺ area fraction was

decreased in DG, suggesting reduced coverage of glutamate transporters in this area (not shown, $p = 0.0241$).

CX43 Expression Is Increased in MS+S CA3

Connexins represent a group of transmembrane proteins that assemble into large, pore forming complexes permeable to a variety of cytoplasmic contents up to 1.5 kDa (Loewenstein, 1981), including ions, metabolites, and purinergic signaling molecules (Loewenstein, 1981).

Disruption of gap junction coupling or aberrant hemichannel signaling may be involved in the pathogenesis of neurological disease with seizure or excitotoxic manifestations such as epilepsy (Bedner et al., 2015; Kekesi et al., 2015; Khan et al., 2016; Deshpande et al., 2017). As expression of CX43, the major connexin isoform expressed by astrocytes, is altered in response to inflammation or demyelination (Brand-Schieber et al., 2005; Markoullis et al., 2014; Masaki, 2015) and inflammatory cytokines increase connexin open probability (Retamal et al., 2007; Froger et al., 2010), CX43 immunostaining was assessed in the HBSFRC cohort.

CX43 staining intensity was comparable between MS & MS+S specimens in the CA1 (Figure 6A and D) and DG (Figure 6C and F). In contrast, CX43 intensity was

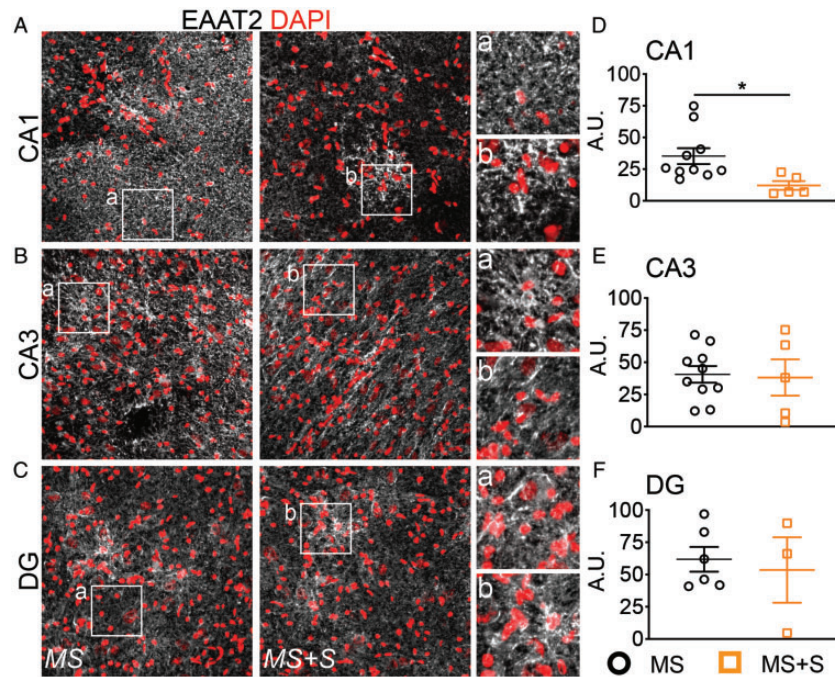


Figure 5. EAAT2 expression is reduced in the CA1 of MS+S specimens obtained from the HBSFRC. A–C: Representative 20X micrographs showing EAAT2 (gray) with nuclear counterstain (DAPI; red) in CA1, CA3, & DG of MS & MS+S hippocampi. Insets a and b show digitally magnified area within dashed boxes for detail. D–F: Normalized EAAT2 immunoreactive signal intensity in MS & MS+S CA1 (D), CA3 (E), and DG (F) shown in arbitrary units (A.U.). Relative to MS, EAAT2+ signal intensity was greater in CA1 of MS+S specimens. No difference was observed in CA3 or DG. Unpaired t test.

elevated in MS+S CA3 relative to MS only (Figure 6B and E). No difference was observed in immunoreactive area fraction in any region analyzed.

Discussion

In the current study, we sought to shed light on the pathogenesis of seizures in MS by examining hippocampi of MS and MS+S donors obtained from the UCLA HBSFRC. Specifically, we assessed changes to astrocytes that could lead to dysregulated neuronal excitation, including expression of molecules associated with synaptic glutamate clearance and spatial K^+ buffering as well as response to inflammation or injury. We found that, although demyelinated lesion burden was comparable among the tissues acquired from the HBSFRC, astrocyte dysfunction in MS+S specimens relative to MS varied by hippocampal subregion (Table 3). Based on these findings, we constructed a model summarizing how our observations could contribute to neuronal hyperexcitability in MS (Figure 7).

Surprisingly, the MS+S CA1 displayed the greatest number of changes compared to the MS group. In addition to GFAP⁺ astrogliosis surpassing that seen in MS, AQP4 and EAAT2 were less robustly expressed in the

MS+S CA1. These phenomena could promote seizures; EAAT2's activity accounts for roughly 95% of synaptic glutamate buffering in the adult mammalian CNS (Bergles & Jahr, 1998). Underscoring the critical role it plays in regulating neuronal excitability, hypofunction mutations to *SLC1A2* are sufficient to generate severe pediatric epilepsy (Guella et al., 2017), with seizure severity depending on the site of lost EAAT2 performance (Sugimoto et al., 2018). Although both neurons and glia express EAAT2 (Danbolt et al., 2016), genetic ablation from neurons results in no gross phenotype, while its loss from astrocytes produces severe behavioral abnormalities and lethal seizures (Petr et al., 2015). Thus, the reduced EAAT2 signal observed in the MS+S CA1 in the present study may increase seizure susceptibility by abnormally bolstering synaptic glutamate concentrations (Figure 7A).

The second way that these data could contribute to seizure vulnerability in MS patients is inferred from the suppression of AQP4 expression seen in the MS+S CA1 & CA3. AQP4 is a passive water channel expressed primarily by astrocytes that is enriched in endfeet contacting blood vessels, which contributes to normal extracellular space volume, glymphatic solute clearance, and K^+ buffering (Mestre et al., 2018). Loss of perivascular AQP4

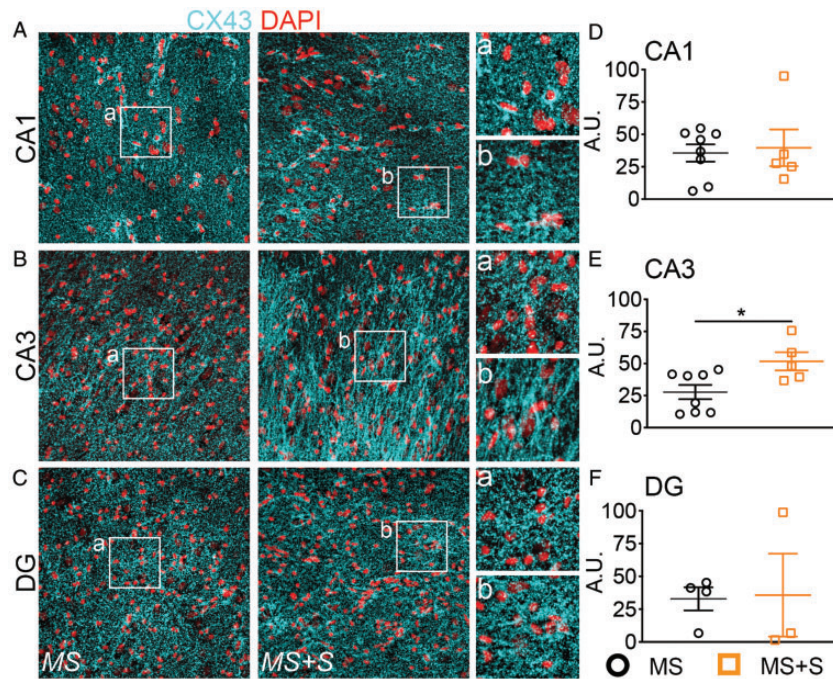


Figure 6. CX43 expression is enhanced in MS+S CA3 within the HBSFRC cohort. A–C: Representative 20X micrographs showing CX43 (cyan) with nuclear counterstain (DAPI; red) in CA1, CA3, & DG of MS & MS+S hippocampi. Insets a & b show digitally magnified area within dashed boxes for detail. D–F: Normalized CX43 immunoreactive signal intensity in MS & MS+S CA1 (D), CA3 (E), and DG in shown in arbitrary units (A.U.). Relative to MS, CX43+ signal intensity was greater in CA3 of MS+S specimens. No difference was observed in CA3 or DG. Unpaired t test.

Table 3. Comparison of Biomarker Expression in MS+S Hippocampal Subregions Versus MS Only.

| Changes in- | CA1 | CA3 | DG |
|------------------------------|-----|-----|----|
| Astrogliosis | ↑ | — | — |
| Water homeostasis | ↓ | ↓ | — |
| Synaptic glutamate clearance | ↓ | — | — |
| Connexin expression | — | ↑ | — |

results in delayed K^+ clearance and protracted stimulation-evoked seizures, potentially leading to hyperexcitability pursuant to loss of K^+ charge separation (Strohschein et al., 2011; Figure 7B). Indeed, AQP4 expression is perturbed throughout epileptic hippocampi, with loss of its normal perivascular distribution in the CA1 (Eid et al., 2005). These observations have parallels in results obtained from the HBSFRC cohort: in addition to the decreased expression noted, perivascular AQP4 expression was sparse in the MS+S CA1, hinting at a role for this molecular in seizure etiology in MS. Of note, seizures are less common in patients with neuromyelitis optica spectrum disorder (NMOSD), a demyelinating disease related to MS characterized by circulating anti-AQP4 IgG, than MS patients (Hamid et al., 2018). As internalization of perivascular AQP4 is

also observed at astrocyte endfeet in NMOSD, the contribution of reduced AQP4 to the genesis of seizures in MS requires additional study (Hinson et al., 2017).

While postmortem studies resist conclusions regarding function, these data suggest MS+S may involve two hits; persistently elevated extracellular K^+ concentration engendered by reduced perivascular AQP4 could lower seizure threshold by mildly depolarizing neurons. Simultaneously, reduced EAAT2 could suppress efficiency of neurotransmission-released glutamate clearance, leading to stronger and more frequent ionotropic glutamate receptor mediated synaptic potentials. Thus, with more glutamatergic neurotransmission and less input needed to elicit an action potential in affected neurons, these data may represent one way that the MS+S CA1 is predisposed to seizure (Figure 7C). Considering that loss of inhibitory neuron populations is also observed in various brain regions during demyelinating disease, GABAergic containment of pathological excitation may be insufficient to stem its spread to neighboring structures (Ziehn et al., 2010).

While these data point to one plausible means of propagating seizures in MS, the finding that CX43 expression is enhanced in the MS+S CA3 raises several questions regarding the nature of such upregulation. In the brain, glia are the foremost expressers of connexin proteins,

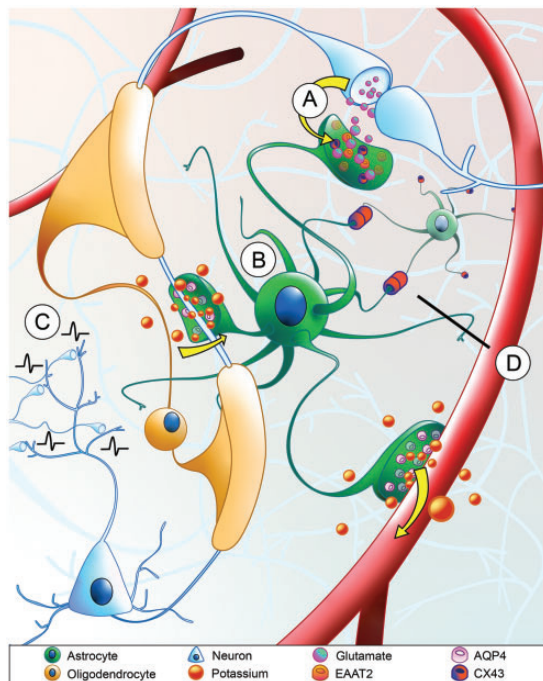


Figure 7. Model summarizing MS+S neuropathology differing from MS only and its impact on neuronal excitability. A: Reduced EAAT2 expression suggests aberrant elevation of synaptic glutamate concentration in MS+S, resulting in protracted, higher amplitude post-synaptic response. B: Decreased AQP4 expression and localization away from blood vessels in MS+S suggests compromised K^+ removal, thereby raising resting membrane potential (RMP) and reducing synaptic input required to initiate action potential. C: Increased synaptic glutamate and more depolarized RMP increase the frequency of synaptic potentials experienced by principle neurons, leading to generation of high amplitude excitatory discharge and seizure. D: Increased CX43 expression in CA3 may represent enhanced gap junction coupling among astrocytes or proliferation of uncoupled hemichannels, rendering its relevance unclear in the context of MS+S.

which link astrocytes and oligodendrocytes into a glial syncytium. This network of interconnected cells facilitates spatial K^+ buffering and propagation of Ca^{2+} waves through gap junction (GJ)-mediated direct cytoplasmic coupling (Lapato & Tiwari-Woodruff, 2018). Additionally, uncoupled connexin hemichannels facing the extracellular space are thought to modulate neurotransmission via release of so-called gliotransmitters, such as purines, D-serine, and glutamate (Durkee & Araque, 2019). In the present study, CX43 expression was increased in MS+S CA3, which has parallels in epileptic brain tissue (Wu et al., 2015), however, whether this represents increased GJ-coupling or hemichannel mobilization cannot be inferred from this study (Figure 7D).

Notably, the finding that demyelinated lesion burden was comparable between HBSFRC cohorts departs from

data published by Calabrese et al. (Calabrese et al., 2017). This is perhaps unsurprising given the small cohort sizes available for each study (23 RRMS patients with seizures were enrolled in (Calabrese et al., 2017) and 7 specimens here). Methodological differences may also contribute to the discrepancy between the two studies. GMLs were identified in (Calabrese et al., 2017) solely by 3 Tesla MRI using a double inversion recovery protocol, whereas here, chromogen immunoreaction and transmitted light microscopy were used. Given the studies' cohort sizes, methodological differences, and the variable extent to which MRI and histology probe the same phenomena, it is difficult to assess whether these studies are in opposition (Xiao et al., 2010; Noristani et al., 2015; Atkinson et al., 2019). Additional investigation is warranted to examine many aspects of seizures in MS and may benefit from comprehensive analysis of the correlation between double inversion recovery MRI and histopathology.

Despite this uncertainty, several scenarios are plausible given our understanding of how inflammatory demyelination affects connexin dynamics. Both oligodendrocyte death and inflammatory cytokines diminish GJ coupling and increase hemichannel open probability (Lapato & Tiwari-Woodruff, 2018). If the increased CX43 observed represents more abundant hemichannels, the proinflammatory cytokine milieu encountered by astrocytes could augment release of glutamatergic and purinergic signaling molecules through hemichannels permeable to the extracellular space (Chever et al., 2014a). In such a case, hemichannel blockade could ameliorate seizures in MS+S, as similar interventions have proven to reduce seizure severity in animal models of epilepsy associated with greater hemichannel activity (Walrave et al., 2018).

An alternative interpretation of increased CX43 pertains to increased GJ coupling in the MS+S CA3. CX43⁺ GJs couple astrocytes to one another and to oligodendrocytes, thereby facilitating movement of K^+ from areas of depolarizing activity to blood vessels for removal (Fasciani et al., 2018). This may, therefore, represent a compensatory mechanism in the seizure prone MS+S hippocampus to address chronically elevated extracellular K^+ concentrations. Lending credence to this possibility, decreased AQP4 expression positively regulates CX43 (Katoozi et al., 2017). While the physiological relevance of such compensation is unclear, reports link connexin-mediated astrocyte synchrony to neuronal burst firing during seizures in acute hippocampal slices (Kekesi et al., 2015). To resolve this question, a greater degree of experimental manipulation is necessary.

The cuprizone (CPZ) model may be useful for studying MS+S. Mice given 0.2% dietary CPZ display behavioral and electrographic seizures (Lapato et al., 2017) that are associated with loss of CA1 inhibitory neurons,

specifically parvalbumin⁺ cells, mirroring cortical MS+S neuropathology (Nicholas et al., 2016). Astrocytes from these mice also exhibit loss of domain organization, membrane varicosities suggestive of energetic failure, and perturbed AQP4 & EAAT2 expression (Lapato et al., 2017). The parallel between these observations and MS+S astrocytes suggests the CPZ model may be translationally useful and future studies should validate this comparison.

Overall, even though MS+S patients represent a minority of the population with MS, the greater morbidity & mortality as well as decreased quality of life in this group behooves further investigation of the pathology, cellular and molecular mechanisms leading to seizures in these patients.

Acknowledgments

The authors would also like to thank Dr. Djurdjica Coss for generously providing access to her Leica DM5500 B transmitted light microscope.

Declaration of Conflicting Interests

The author(s) declared no potential conflicts of interest with respect to the research, authorship, and/or publication of this article.

Funding

The author(s) disclosed receipt of the following financial support for the research, authorship, and/or publication of this article: This work was supported by National Institutes of Health Grants NMSS Pilot Grant, PP-1609-25942, NIH R01NS081141 and NIH R01NS111552 to STW. Human tissue was received from the NIH NeuroBioBank at the Human Brain and Spinal Fluid Resource Center: <http://brainbank.ucla.edu>.

ORCID iD

Seema K. Tiwari-Woodruff  <https://orcid.org/0000-0001-7608-4763>

Supplemental Material

Supplemental material for this article is available online.

References

- Alvestad, S., Hammer, J., Hoddevik, E. H., Skare, O., Sonnewald, U., Amiry-Moghaddam, M., & Ottersen, O. P. (2013). Mislocalization of AQP4 precedes chronic seizures in the Kainate model of temporal lobe epilepsy. *Epilepsy Research, 105*(1–2), 30–41.
- Atkinson, K. C., Lee, J. B., Hasselmann, J. P. C., Kim, S. H., Drew, A., Soto, J., Katzenellenbogen, J. A., Harris, N. G., Obenaus, A., & Tiwari-Woodruff, S. K. (2019). Diffusion tensor imaging identifies aspects of therapeutic estrogen receptor beta ligand-induced remyelination in a mouse model of multiple sclerosis. *Neurobiology of Disease, 130*, 104501.
- Azevedo, C. J., Kornak, J., Chu, P., Sampat, M., Okuda, D. T., Cree, B. A., Nelson, S. J., Hauser, S. L., & Pelletier, D. (2014). In vivo evidence of glutamate toxicity in multiple sclerosis. *Annals of Neurology, 76*(2), 269–278.
- Bedner, P., & Steinhauser, C. (2013). Altered kir and gap junction channels in temporal lobe epilepsy. *Neurochemistry International, 63*(7), 682–687.
- Bedner, P., Dupper, A., Huttmann, K., Muller, J., Herde, M. K., Dublin, P., Deshpande, T., Schramm, J., Haussler, U., Haas, C. A., Henneberger, C., Theis, M., & Steinhauser, C. (2015). Astrocyte uncoupling as a cause of human temporal lobe epilepsy. *Brain: A Journal of Neurology, 138*(Pt 5), 1208–1222.
- Bergles, D. E., & Jahr, C. E. (1998). Glial contribution to glutamate uptake at Schaffer collateral-commissural synapses in the hippocampus. *The Journal of Neuroscience: The Official Journal of the Society for Neuroscience, 18*(19), 7709–7716.
- Binder, D. K., Yao, X., Zador, Z., Sick, T. J., Verkman, A. S., & Manley, G. T. (2006). Increased seizure duration and slowed potassium kinetics in mice lacking aquaporin-4 water channels. *Glia, 53*(6), 631–636.
- Brand-Schieber, E., Werner, P., Iacobas, D. A., Iacobas, S., Beelitz, M., Lowery, S. L., Spray, D. C., & Scemes, E. (2005). Connexin43, the major gap junction protein of astrocytes, is down-regulated in inflamed white matter in an animal model of multiple sclerosis. *Journal of Neuroscience Research, 80*(6), 798–808.
- Brosnan, C. F., & Raine, C. S. (2013). The astrocyte in multiple sclerosis revisited. *Glia, 61*(4), 453–465.
- Burman, J., & Zelano, J. (2017). Epilepsy in multiple sclerosis: A nationwide population-based register study. *Neurology, 89*(24), 2462–2468.
- Calabrese, M., Bernardi, V., Atzori, M., Mattisi, I., Favaretto, A., Rinaldi, F., Perini, P., & Gallo, P. (2012). Effect of disease-modifying drugs on cortical lesions and atrophy in relapsing-remitting multiple sclerosis. *Multiple Sclerosis Journal, 18*(4), 418–424.
- Calabrese, M., Castellaro, M., Bertoldo, A., De Luca, A., Pizzini, F. B., Ricciardi, G. K., Pitteri, M., Zimatore, S., Magliozzi, R., Benedetti, M. D., Manganotti, P., Montemezzi, S., Reynolds, R., Gajofatto, A., & Monaco, S. (2017). Epilepsy in multiple sclerosis: The role of temporal lobe damage. *Multiple Sclerosis Journal, 23*(3), 473–482.
- Calabrese, M., De Stefano, N., Atzori, M., Bernardi, V., Mattisi, I., Barachino, L., Rinaldi, L., Morra, A., McAuliffe, M. M., Perini, P., Battistin, L., & Gallo, P. (2008). Extensive cortical inflammation is associated with epilepsy in multiple sclerosis. *Journal of Neurology, 255*(4), 581–586.
- Catenoix, H., Marignier, R., Ritleng, C., Dufour, M., Mauguier, F., Confavreux, C., & Vukusic, S. (2011). Multiple sclerosis and epileptic seizures. *Multiple Sclerosis Journal, 17*(1), 96–102.
- Chever, O., Lee, C. Y., & Rouach, N. (2014a). Astroglial connexin43 hemichannels tune basal excitatory synaptic

- transmission. *The Journal of Neuroscience: The Official Journal of the Society for Neuroscience*, 34(34), 11228–11232.
- Chever, O., Pannasch, U., Ezan, P., & Rouach, N. (2014b). Astroglial connexin 43 sustains glutamatergic synaptic efficacy. *Philosophical Transactions of the Royal Society of London. Series B, Biological Sciences*, 369(1654), 20130596.
- Colasanti, A., Guo, Q., Giannetti, P., Wall, M. B., Newbould, R. D., Bishop, C., Onega, M., Nicholas, R., Ciccarelli, O., Muraro, P. A., Malik, O., Owen, D. R., Young, A. H., Gunn, R. N., Piccini, P., Matthews, P. M., & Rabiner, E. A. (2016). Hippocampal neuroinflammation, functional connectivity, and depressive symptoms in multiple sclerosis. *Biological Psychiatry*, 80(1), 62–72.
- Coulter, D. A., & Steinhauser, C. (2015). Role of astrocytes in epilepsy. *Cold Spring Harbor Perspectives in Medicine*, 5(3), a022434.
- Crawford, D. K., Mangiardi, M., Song, B., Patel, R., Du, S., Sofroniew, M. V., Voskuhl, R. R., & Tiwari-Woodruff, S. K. (2010). Oestrogen receptor beta ligand: A novel treatment to enhance endogenous functional remyelination. *Brain: A Journal of Neurology*, 133(10), 2999–3016.
- Danbolt, N. C., Furness, D. N., & Zhou, Y. (2016). Neuronal vs glial glutamate uptake: Resolving the conundrum. *Neurochemistry International*, 98, 29–45.
- de Lanerolle, N. C., Lee TS., & Spencer DD. (2012). Histopathology of human epilepsy. In: *Jasper's basic mechanisms of the epilepsies* (4th ed., Noebels JL, Avoli M, Rogawski MA, Olsen RW, Delgado-Escueta AV, eds). National Center for Biotechnology Information (US).
- Deshpande, T., Li, T., Herde, M. K., Becker, A., Vatter, H., Schwarz, M. K., Henneberger, C., Steinhauser, C., & Bedner, P. (2017). Subcellular reorganization and altered phosphorylation of the astrocytic gap junction protein connexin43 in human and experimental temporal lobe epilepsy. *Glia*, 65(11), 1809–1820.
- Durkee, C. A., & Araque, A. (2019). Diversity and specificity of astrocyte-neuron communication. *Neuroscience*, 396, 73–78.
- Eid, T., Lee, T. S., Thomas, M. J., Amiry-Moghaddam, M., Bjornsen, L. P., Spencer, D. D., Agre, P., Ottersen, O. P., & de Lanerolle, N. C. (2005). Loss of perivascular aquaporin 4 may underlie deficient water and K⁺ homeostasis in the human epileptogenic hippocampus. *Proceedings of the National Academy of Sciences of the United States of America*, 102(4), 1193–1198.
- Fasciani, I., Pluta, P., Gonzalez-Nieto, D., Martinez-Montero, P., Molano, J., Paino, C. L., Millet, O., & Barrio, L. C. (2018). Directional coupling of oligodendrocyte connexin-47 and astrocyte connexin-43 gap junctions. *Glia*, 66(11), 2340–2352.
- Froger, N., Orellana, J. A., Calvo, C. F., Amigou, E., Kozoriz, M. G., Naus, C. C., Saez, J. C., & Giaume, C. (2010). Inhibition of cytokine-induced connexin43 hemichannel activity in astrocytes is neuroprotective. *Molecular and Cellular Neurosciences*, 45(1), 37–46.
- Gavillet, M., Allaman, I., & Magistretti, P. J. (2008). Modulation of astrocytic metabolic phenotype by proinflammatory cytokines. *Glia*, 56(9), 975–989.
- Ghezzi, A., Montanini, R., Basso, P. F., Zaffaroni, M., Massimo, E., & Cazzullo, C. L. (1990). Epilepsy in multiple sclerosis. *European Neurology*, 30(4), 218–223.
- Guella, I., McKenzie, M. B., Evans, D. M., Buerki, S. E., Toyota, E. B., Van Allen, M. I., Epilepsy Genomics, S., Suri, M., Elmslie, F., Deciphering Developmental Disorders, S., Simon, M. E. H., van Gassen, K. L. I., Heron, D., Keren, B., Nava, C., Connolly, M. B., Demos, M., Farrer, M. J., & Deciphering Developmental Disorders Study. (2017). De novo mutations in YWHAG cause early-onset epilepsy. *American Journal of Human Genetics*, 101(2), 300–310.
- Hamid, S. H. M., Whittam, D., Saviour, M., Alorainy, A., Mutch, K., Linaker, S., Solomon, T., Bhojak, M., Woodhall, M., Waters, P., Appleton, R., Duddy, M., & Jacob, A. (2018). Seizures and encephalitis in myelin oligodendrocyte glycoprotein IgG disease vs aquaporin 4 IgG disease. *JAMA Neurology*, 75(1), 65–71.
- Hasselmann, J. P., Karim, H., Khalaj, A. J., Ghosh, S., & Tiwari-Woodruff, S. K. (2017). Consistent induction of chronic experimental autoimmune encephalomyelitis in C57BL/6 mice for the longitudinal study of pathology and repair. *Journal of Neuroscience Methods*, 284, 71–84.
- Hinson, S. R., Clift, I. C., Luo, N., Kryzer, T. J., & Lennon, V. A. (2017). Autoantibody-induced internalization of CNS AQP4 water channel and EAAT2 glutamate transporter requires astrocytic Fc receptor. *Proceedings of the National Academy of Sciences of the United States of America*, 114(21), 5491–5496.
- Holmseth, S., Scott, H. A., Real, K., Lehre, K. P., Leergaard, T. B., Bjaalie, J. G., & Danbolt, N. C. (2009). The concentrations and distributions of three C-terminal variants of the GLT1 (EAAT2; slc1a2) glutamate transporter protein in rat brain tissue suggest differential regulation. *Neuroscience*, 162(4), 1055–1071.
- Hubbard, J. A., Szu, J. I., Yonan, J. M., & Binder, D. K. (2016). Regulation of astrocyte glutamate transporter-1 (GLT1) and aquaporin-4 (AQP4) expression in a model of epilepsy. *Experimental Neurology*, 283(Pt A), 85–96.
- Huusko, N., Romer, C., Ndode-Ekane, X. E., Lukasiuk, K., & Pitkanen, A. (2015). Loss of hippocampal interneurons and epileptogenesis: A comparison of two animal models of acquired epilepsy. *Brain Structure and Function*, 220(1), 153–191.
- Karim, H., Kim, S. H., Lapato, A. S., Yasui, N., Katzenellenbogen, J. A., & Tiwari-Woodruff, S. K. (2018). Increase in chemokine CXCL1 by ERbeta ligand treatment is a key mediator in promoting axon myelination. *Proceedings of the National Academy of Sciences*, 115(24), 6291–6296.
- Katozi, S., Skauli, N., Rahmani, S., Camassa, L. M. A., Boldt, H. B., Ottersen, O. P., & Amiry-Moghaddam, M. (2017). Targeted deletion of Aqp4 promotes the formation of astrocytic gap junctions. *Brain Structure & Function*, 222(9), 3959–3972.
- Kekesi, O., Ioja, E., Szabo, Z., Kardos, J., & Heja, L. (2015). Recurrent seizure-like events are associated with coupled astroglial synchronization. *Frontiers in Cellular Neuroscience*, 9, 215.

- Kelley, B. J., & Rodriguez, M. (2009). Seizures in patients with multiple sclerosis: Epidemiology, pathophysiology and management. *CNS Drugs*, 23(10), 805–815.
- Khan, D., Dupper, A., Deshpande, T., Graan, P. N., Steinhäuser, C., & Bedner, P. (2016). Experimental febrile seizures impair interastrocytic gap junction coupling in juvenile mice. *Journal of Neuroscience Research*, 94(9), 804–813.
- Koch, M., Uyttenboogaart, M., Polman, S., & De Keyser, J. (2008). Seizures in multiple sclerosis. *Epilepsia*, 49(6), 948–953.
- Lapato, A. S., & Tiwari-Woodruff, S. K. (2018). Connexins and pannexins: At the junction of neuro-glial homeostasis & disease. *Journal of Neuroscience Research*, 96(1), 31–44.
- Lapato, A. S., Szu, J. I., Hasselmann, J. P. C., Khalaj, A. J., Binder, D. K., & Tiwari-Woodruff, S. K. (2017). Chronic demyelination-induced seizures. *Neuroscience*, 346, 409–422.
- Lee, D. J., Amini, M., Hamamura, M. J., Hsu, M. S., Seldin, M. M., Nalcioğlu, O., & Binder, D. K. (2012b). Aquaporin-4-dependent edema clearance following status epilepticus. *Epilepsy Research*, 98(2–3), 264–268.
- Lee, D. J., Hsu, M. S., Seldin, M. M., Arellano, J. L., & Binder, D. K. (2012a). Decreased expression of the glial water channel aquaporin-4 in the intrahippocampal kainic acid model of epileptogenesis. *Experimental Neurology*, 235(1), 246–255.
- Lee, T. S., Eid, T., Mane, S., Kim, J. H., Spencer, D. D., Ottersen, O. P., & de Lanerolle, N. C. (2004). Aquaporin-4 is increased in the sclerotic hippocampus in human temporal lobe epilepsy. *Acta Neuropathologica*, 108(6), 493–502.
- Lehre, K. P., & Danbolt, N. C. (1998). The number of glutamate transporter subtype molecules at glutamatergic synapses: Chemical and stereological quantification in young adult rat brain. *The Journal of Neuroscience: The Official Journal of the Society for Neuroscience*, 18(21), 8751–8757.
- Loewenstein, W. R. (1981). Junctional intercellular communication: The cell-to-cell membrane channel. *Physiological Reviews*, 61(4), 829–913.
- Lund, C., Nakken, K. O., Edland, A., & Celius, E. G. (2014). Multiple sclerosis and seizures: Incidence and prevalence over 40 years. *Acta Neurologica Scandinavica*, 130(6), 368–373.
- Mangiardi, M., Crawford, D. K., Xia, X., Du, S., Simon-Freeman, R., Voskuhl, R. R., & Tiwari-Woodruff, S. K. (2011). An animal model of cortical and callosal pathology in multiple sclerosis. *Brain Pathology (Zurich, Switzerland)*, 21(3), 263–278.
- Markoullis, K., Sargiannidou, I., Schiza, N., Roncaroli, F., Reynolds, R., & Kleopa, K. A. (2014). Oligodendrocyte gap junction loss and disconnection from reactive astrocytes in multiple sclerosis gray matter. *Journal of Neuropathology and Experimental Neurology*, 73(9), 865–879.
- Martínez-Juárez, I. E., López-Meza, E., González-Aragón, M. d. C. F., Ramírez-Bermúdez, J., & Corona, T. (2009). Epilepsy and multiple sclerosis: Increased risk among progressive forms. *Epilepsy Research*, 84(2–3), 250–253.
- Martinez-Lapiscina, E. H., Ayuso, T., Lacruz, F., Gurtubay, I. G., Soriano, G., Otano, M., Bujanda, M., & Bacaicoa, M. C. (2013). Cortico-juxtacortical involvement increases risk of epileptic seizures in multiple sclerosis. *Acta Neurologica Scandinavica*, 128(1), 24–31.
- Masaki, K. (2015). Early disruption of glial communication via connexin gap junction in multiple sclerosis, Balo's disease and neuromyelitis optica. *Neuropathology: Official Journal of the Japanese Society of Neuropathology*, 35(5), 469–480.
- Mathern, G. W., Mendoza, D., Lozada, A., Pretorius, J. K., Dehnes, Y., Danbolt, N. C., Nelson, N., Leite, J. P., Chimelli, L., Born, D. E., Sakamoto, A. C., Assirati, J. A., Fried, I., Peacock, W. J., Ojemann, G. A., & Adelson, P. D. (1999). Hippocampal GABA and glutamate transporter immunoreactivity in patients with temporal lobe epilepsy. *Neurology*, 52(3), 453–472.
- Mestre, H., Hablitz, L. M., Xavier, A. L., Feng, W., Zou, W., Pu, T., Monai, H., Murlidharan, G., Castellanos Rivera, R. M., Simon, M. J., Pike, M. M., Plá, V., Du, T., Kress, B. T., Wang, X., Plog, B. A., Thrane, A. S., Lundgaard, I., Abe, Y., . . . Nedergaard, M. (2018). Aquaporin-4-dependent glymphatic solute transport in the rodent brain. *eLife*, 7, e40070.
- Moreau, T., Sochurkova, D., Lemesle, M., Madinier, G., Billiar, T., Giroud, M., & Dumas, R. (1998). Epilepsy in patients with multiple sclerosis: Radiological-clinical correlations. *Epilepsia*, 39(8), 893–896.
- Nave, K. A., & Trapp, B. D. (2008). Axon-glial signaling and the glial support of axon function. *Annual Review of Neuroscience*, 31, 535–561.
- Newman, P., & Saunders, M. (1980). A unique case of musicogenic epilepsy. *Archives of Neurology*, 37(4), 244–245.
- Nicholas, R., Magliozzi, R., Campbell, G., Mahad, D., & Reynolds, R. (2016). Temporal lobe cortical pathology and inhibitory GABA interneuron cell loss are associated with seizures in multiple sclerosis. *Multiple Sclerosis Journal*, 22(1), 25–35.
- Noristani, H. N., Lonjon, N., Cardoso, M., Le Corre, M., Chan-Seng, E., Captier, G., Privat, A., Coillot, C., Goze-Bac, C., & Perrin, F. E. (2015). Correlation of in vivo and ex vivo (1)H-MRI with histology in two severities of mouse spinal cord injury. *Frontiers in Neuroanatomy*, 9, 24.
- Nyquist, P. A., Cascino, G. D., & Rodriguez, M. (2001). Seizures in patients with multiple sclerosis seen at Mayo Clinic, Rochester, Minn, 1990–1998. *Mayo Clinic Proceedings*, 76(10), 983–986.
- Petr, G. T., Sun, Y., Frederick, N. M., Zhou, Y., Dhamne, S. C., Hameed, M. Q., Miranda, C., Bedoya, E. A., Fischer, K. D., Armsen, W., Wang, J., Danbolt, N. C., Rotenberg, A., Aoki, C. J., & Rosenberg, P. A. (2015). Conditional deletion of the glutamate transporter GLT-1 reveals that astrocytic GLT-1 protects against fatal epilepsy while neuronal GLT-1 contributes significantly to glutamate uptake into synaptosomes. *The Journal of Neuroscience: The Official Journal of the Society for Neuroscience*, 35(13), 5187–5201.
- Poser, C. M., & Brinar, V. V. (2003). Epilepsy and multiple sclerosis. *Epilepsy & Behavior: E&B*, 4(1), 6–12.
- Preibisch, S., Saalfeld, S., & Tomancak, P. (2009). Globally optimal stitching of tiled 3D microscopic image acquisitions. *Bioinformatics (Oxford, England)*, 25(11), 1463–1465.

- Primavera, A., Gianelli, M. V., & Bandini, F. (1996). Aphasic status epilepticus in multiple sclerosis. *European Neurology*, 36(6), 374–377.
- Proper, E. A., Hoogland, G., Kappen, S. M., Jansen, G. H., Rensen, M. G., Schrama, L. H., van Veelen, C. W., van Rijen, P. C., van Nieuwenhuizen, O., Gispen, W. H., & de Graan, P. N. (2002). Distribution of glutamate transporters in the hippocampus of patients with pharmaco-resistant temporal lobe epilepsy. *Brain: A Journal of Neurology*, 125(Pt 1), 32–43.
- Retamal, M. A., Froger, N., Palacios-Prado, N., Ezan, P., Saez, P. J., Saez, J. C., & Giaume, C. (2007). Cx43 hemichannels and gap junction channels in astrocytes are regulated oppositely by proinflammatory cytokines released from activated microglia. *The Journal of Neuroscience: The Official Journal of the Society for Neuroscience*, 27(50), 13781–13792.
- Rimmele, T. S., & Rosenberg, P. A. (2016). GLT-1: The elusive presynaptic glutamate transporter. *Neurochemistry International*, 98, 19–28.
- Rosenthal, J. F., Hoffman, B. M., & Tyor, W. R. (2020). CNS inflammatory demyelinating disorders: MS, NMOSD and MOG antibody associated disease. *Journal of Investigative Medicine: The Official Publication of the American Federation for Clinical Research*, 68(2), 321–330.
- Schindelin, J., Arganda-Carreras, I., Frise, E., Kaynig, V., Longair, M., Pietzsch, T., Preibisch, S., Rueden, C., Saalfeld, S., Schmid, B., Tinevez, J. Y., White, D. J., Hartenstein, V., Eliceiri, K., Tomancak, P., & Cardona, A. (2012). Fiji: An open-source platform for biological-image analysis. *Nature Methods*, 9(7), 676–682.
- Shaygannejad, V., Ashtari, F., Zare, M., Ghasemi, M., Norouzi, R., & Maghzi, H. (2013). Seizure characteristics in multiple sclerosis patients. *Journal of Research in Medical Sciences: The Official Journal of Isfahan University of Medical Sciences*, 18(Suppl 1), S74–S77.
- Solaro, C., Brichetto, G., Battaglia, M. A., Messmer Uccelli, M., & Mancardi, G. L. (2005). Antiepileptic medications in multiple sclerosis: Adverse effects in a three-year follow-up study. *Neurological Sciences: Official Journal of the Italian Neurological Society and of the Italian Society of Clinical Neurophysiology*, 25(6), 307–310.
- Spatt, J., Chaix, R., & Mamoli, B. (2001). Epileptic and non-epileptic seizures in multiple sclerosis. *Journal of Neurology*, 248(1), 2–9.
- Spatt, J., Goldenberg, G., & Mamoli, B. (1994). Simple dysphasic seizures as the sole manifestation of relapse in multiple sclerosis. *Epilepsia*, 35(6), 1342–1345.
- Striano, P., Orefice, G., Brescia Morra, V., Boccella, P., Sarappa, C., Lanzillo, R., Vacca, G., & Striano, S. (2003). Epileptic seizures in multiple sclerosis: Clinical and EEG correlations. *Neurological Sciences: Official Journal of the Italian Neurological Society and of the Italian Society of Clinical Neurophysiology*, 24(5), 322–328.
- Strohschein, S., Huttmann, K., Gabriel, S., Binder, D. K., Heinemann, U., & Steinhauser, C. (2011). Impact of aquaporin-4 channels on K⁺ buffering and gap junction coupling in the hippocampus. *Glia*, 59(6), 973–980.
- Sugimoto, J., Tanaka, M., Sugiyama, K., Ito, Y., Aizawa, H., Soma, M., Shimizu, T., Mitani, A., & Tanaka, K. (2018). Region-specific deletions of the glutamate transporter GLT1 differentially affect seizure activity and neurodegeneration in mice. *Glia*, 66(4), 777–788.
- Takahashi, D. K., Vargas, J. R., & Wilcox, K. S. (2010). Increased coupling and altered glutamate transport currents in astrocytes following kainic-acid-induced status epilepticus. *Neurobiology of Disease*, 40(3), 573–585.
- Tiwari-Woodruff, S., Morales, L. B., Lee, R., & Voskuhl, R. R. (2007). Differential neuroprotective and antiinflammatory effects of estrogen receptor (ER)alpha and ERbeta ligand treatment. *Proceedings of the National Academy of Sciences of the United States of America*, 104(37), 14813–14818.
- Trapp, B. D., Peterson, J., Ransohoff, R. M., Rudick, R., Mork, S., & Bo, L. (1998). Axonal transection in the lesions of multiple sclerosis. *The New England Journal of Medicine*, 338(5), 278–285.
- Tress, O., Maglione, M., May, D., Pivneva, T., Richter, N., Seyfarth, J., Binder, S., Zlomuzica, A., Seifert, G., Theis, M., Dere, E., Kettenmann, H., & Willecke, K. (2012). Panglial gap junctional communication is essential for maintenance of myelin in the CNS. *The Journal of Neuroscience: The Official Journal of the Society for Neuroscience*, 32(22), 7499–7518.
- Uribe-San-Martin, R., Ciampi-Diaz, E., Suarez-Hernandez, F., Vasquez-Torres, M., Godoy-Fernandez, J., & Carcamo-Rodriguez, C. (2014). Prevalence of epilepsy in a cohort of patients with multiple sclerosis. *Seizure*, 23, 81–83.
- Vercellino, M., Merola, A., Piacentino, C., Votta, B., Capello, E., Mancardi, G. L., Mutani, R., Giordana, M. T., & Cavalla, P. (2007). Altered glutamate reuptake in relapsing-remitting and secondary progressive multiple sclerosis cortex: Correlation with microglia infiltration, demyelination, and neuronal and synaptic damage. *Journal of Neuropathology and Experimental Neurology*, 66(8), 732–739.
- Wallin, M. T., Culpepper, W. J., Campbell, J. D., Nelson, L. M., Langer-Gould, A., Marrie, R. A., Cutter, G. R., Kaye, W. E., Wagner, L., Tremlett, H., Buka, S. L., Dilokthornsakul, P., Topol, B., Chen, L. H., LaRocca, N. G., & US Multiple Sclerosis Prevalence Workgroup. (2019). The prevalence of MS in the United States: A population-based estimate using health claims data. *Neurology*, 92(10), e1029–e1040.
- Walrave, L., Pierre, A., Albertini, G., Aourz, N., De Bundel, D., Van Eeckhaut, A., Vinken, M., Giaume, C., Leybaert, L., & Smolders, I. (2018). Inhibition of astroglial connexin43 hemichannels with TAT-Gap19 exerts anticonvulsant effects in rodents. *Glia*, 66(8), 1788–1804.
- Werner, P., Pitt, D., & Raine, C. S. (2001). Multiple sclerosis: Altered glutamate homeostasis in lesions correlates with oligodendrocyte and axonal damage. *Annals of Neurology*, 50(2), 169–180.
- Wojtowicz, J. M. (2012). Adult neurogenesis. From circuits to models. *Behavioural Brain Research*, 227(2), 490–496.
- Wu, X. L., Tang, Y. C., Lu, Q. Y., Xiao, X. L., Song, T. B., & Tang, F. R. (2015). Astrocytic Cx 43 and Cx 40 in the mouse

- hippocampus during and after pilocarpine-induced status epilepticus. *Experimental Brain Research*, 233(5), 1529–1539.
- Xiao, J., Wong, A. W., Willingham, M. M., van den Buuse, M., Kilpatrick, T. J., & Murray, S. S. (2010). Brain-derived neurotrophic factor promotes central nervous system myelination via a direct effect upon oligodendrocytes. *Neuro-Signals*, 18(3), 186–202.
- Ziehn, M. O., Avedisian, A. A., Tiwari-Woodruff, S., & Voskuhl, R. R. (2010). Hippocampal CA1 atrophy and synaptic loss during experimental autoimmune encephalomyelitis, EAE. *Laboratory Investigation: A Journal of Technical Methods and Pathology*, 90(5), 774–786.